NASA/CR—1999-206592

Survey of Turbulence Models for the Computation of Turbulent Jet Flow and Noise

M. Nallasamy
Dynacs Engineering Co., Brook Park, Ohio

Prepared under Contract NAS3–98008

National Aeronautics and
Space Administration

Glenn Research Center

March 1999

Available from

NASA Center for Aerospace Information
7121 Standard Drive
Hanover, MD 21076
Price Code: A03

National Technical Information Service
5285 Port Royal Road
Springfield, VA 22100
Price Code: A03

TABLE OF CONTENTS

NOMENCLATURE

c	speed of sound
D	jet diameter
c_ε	turbulence model coefficients
f, f'	ean and fluctuating components of variable f
g	time factor (Eq. 41)
k	turbulence kinetic energy, $\frac{1}{2}\overline{u_i u_i}$
l	turbulence length scale
M_t	turbulent Mach number, Eq. 23.
P_{ij}	stress production, Eq. 6, $P = P_{kk}/2$
p	pressure
R	radius
R_g	gas constant
R_{ij}	space factor, Eq. 41.
R_t	turbulence Reynolds number
T	temperature
T_{ij}	Lighthill stress tensor
u,v,w	fluctuating velocities in x,y,z directions
u_τ	friction velocity
x,y,z	Cartesian coordinates
y^+	nondimensonal distance, yu_τ/ν
α	factor in Sarkar compressbility correction, Eq. 23 & 43
β	factor in compressible dissiapation model, Eq. 43
δ_{ij}	Kronecker delta
ε	dissipation rate of turbulence energy
γ	ratio of specific heats
λ	factor in Zeman compressibility correction, Eq. 43
μ	dynamic viscosity

ν	kinematic viscosity
ν_t	turbulent viscosity
θ	polar coordinate
ρ	density
σ	turbulent Prandtl number for diffusion of k and ε
τ_ω	characteristic time dalay
τ_τ	shear stress
Ω	source frequency

SURVEY OF TURBULENCE MODELS FOR THE COMPUTATION OF TURBULENT JET FLOW AND NOISE

Abstract

The report presents an overview of jet noise computation utilizing the computational fluid dynamic solution of the turbulent jet flow field. The jet flow solution obtained with an appropriate turbulence model provides the turbulence characteristics needed for the computation of jet mixing noise. A brief account of turbulence models that are relevant for the jet noise computation is presented. The jet flow solutions that have been directly used to calculate jet noise are first reviewed. Then, the turbulent jet flow studies that compute the turbulence characteristics that may be used for noise calculations are summarized. In particular, flow solutions obtained with the k-ε model, algebraic Reynolds stress model, and Reynolds stress transport equation model are reviewed. Since, the small scale jet mixing noise predictions can be improved by utilizing anisotropic turbulence characteristics, turbulence models that can provide the Reynolds stress components must now be considered for jet flow computations. In this regard, algebraic stress models and Reynolds stress transport models are good candidates. Reynolds stress transport models involve more modeling and computational effort and time compared to algebraic stress models. Hence, it is recommended that an algebraic Reynolds stress model (ASM) be implemented in flow solvers to compute the Reynolds stress components.

I. INTRODUCTION

The study of the origin of jet noise began around 1950 in response to the then emerging need to control the noise of jet propelled aircraft. Lighthill [1,2] proposed the theory of aerodynamic sound to describe the mechanism of noise generation from the mixing zone of turbulent jets. It is an exact formulation based on the fundamental equations of fluid motion. Lighthill's equation for density fluctuations in a flow is written as,

$$\frac{\partial^2 \rho'}{\partial t^2} - c^2 \nabla^2 \rho' = \frac{\partial^2 T_{ij}}{\partial x_i x_j} \tag{1}$$

where

$$T_{ij} = \rho u_i u_j - \tau_{ij} + (p - \rho c^2)\delta_{ij} \tag{2}$$

is the Lighthill stress tensor.

The theory replaces the actual flow by a flow at rest with an acoustic field in which waves propagate at constant speed c. The source field for the waves is a quadrupole distribution and the strength of the quadrupole in unit volume is given by Lihgthill stress tensor, T_{ij}. The double divergence on T_{ij} indicates that the source is a quadrupole. Thus in Lighthill's analogy the sources move instead of the fluid. Hence if T_{ij} is known throughout the real flow field the wave equation (1) can be solved, to evaluate the small scale jet mixing noise.

In the absence of a detailed flow field solution, simple scaling laws derived for the turbulent flow were used to estimate the sound radiation from turbulent jets. Such estimates showed poor agreement with the data. The variation of sound spectra with angle to the jet axis was poorly estimated at moderate and high frequencies. This was traced to the neglect of mean flow effects on the radiated field. Lilley [3] formulated the jet noise problem in terms of jet noise generation and sound-flow interaction, accounting for the effect of refraction and convection. This formulation is used in a majority of recent investigations of jet noise.

The problem of estimating the distribution of T_{ij} throughout the flow field has been the subject of numerous investigations. A fully time dependent numerical simulation (Direct Numerical Simulation, DNS) of the turbulent jet flow can be used to provide the distribution of noise source strength T_{ij}. But such full simulations are still restricted to simple flows and low Mach numbers. Colonious et al [4] computed the acoustic field due to plane mixing layer, using direct simulation. Before we look for other methods of computing T_{ij}, let us look at the terms in Lighthill stress tensor. The first term $\rho u_i u_j$ is the momentum flux per unit volume. The second term $-\tau_{ij}$ is the viscous stress, which can be neglected for high Reynolds number flows. The third term $(p - \rho c^2)\delta_{ij}$ is normally considered to be small order compared to $\rho u_i u_j$ in isentropic flows, where the temperature difference between the flow and the ambient is small. So for majority of the flows of interest $T_{ij} = \rho u_i u_j$. $\rho u_i u_j$ is the unsteady Reynolds stress. However, the full space-time history of T_{ij} can not easily be evaluated for flows of practical interest..

The Reynolds stress distribution can be obtained from the solution of Reynolds averaged Navier-Stokes (RANS) equations. Substitution of apparent mean (Reynolds) stresses for the actual transfer of momentum by the velocity fluctuations increase the number of unknowns above the number of equations. The problem then is to supply the information missing from the time-averaged equations by formulating a model to describe some or all of the six independent Reynolds stresses, $-\overline{\rho u_i u_j}$. The exact Reynolds stress transport equations can be derived from the time dependent Navier-Stokes equations [5]. These equations express the conservation of each Reynolds stress as the Navier-Stokes equations express the conservation of each component of momentum. In turbulence modeling one uses a finite number of Reynolds stress transport equations and supplies missing information from experimental (or analytical) results. The time-averaged scalar transport equation contains the turbulent heat or mass flux, $-\overline{\rho u_i \phi}$, where ϕ is the fluctuating scalar quantity. When only time averaged information is available, modeling

of the turbulent velocity frequency–wave number spectrum is required to obtain noise spectra as a function of directivity angle.

From a time averaged solution with appropriate turbulence modeling, turbulence length and time scales needed for the acoustic solution can be extracted. This approach has been adopted by Khavaran et al [6], Bailey et al [7,8], and Khavaran and Krejsa [9] recently to compute the sound radiated from turbulent jets. These papers use k-ε turbulence models and they express the turbulence length and time scales in terms of turbulent kinetic energy, k, and its dissipation rate, ε. In this report, we will look at the turbulence models that provide k and ε, for use in noise calculations.

Several reviews of turbulence models have appeared concentrating on different aspects of turbulence modeling [for example, 10 –15]. A recent review by Hanjalic [16] summarizes the applications of single point closure methods and discusses possible directions for turbulence model improvements. Spieziale [17] discusses mathematical aspects of Reynolds stress closure methods. The book (revised, 2nd Edition) by Wilcox [18] contains complete details of turbulence models that are employed in computational fluid dynamics computations.

One recent NASA conference publication [19] presents various turbulence models and their applications to subsonic/supersonic flows, wall bounded and free shear flows of interest in propulsion. Turbulence models used by various industries and research organizations and the results obtained with these models are presented. In another NASA/Industry report [20] nozzle flow computational results obtained from five different codes (from GE, UTRC, MDC, Boeing, and Glenn Research Center (GRC)) with different models were evaluated. The codes were found to produce similar results when they used common grids, boundary conditions, and turbulence models. The results showed little sensitivity to upstream turbulence levels, but showed strong dependence on the choice of turbulence model and the near wall treatment.

In the present survey, we examine the turbulence models that are relevant for the computation of jet flow for the purpose of evaluating sound radiated from turbulent jets. First a description of turbulence models which are relevant for computing the noise radiated by jets is given. Then the application of the models and their performance in jet flows of interest are described.

II. TURBULENCE MODELS

The transport equations for the Reynolds stress tensor can be derived from Navier-Stokes equations [5]. Since such transport equations contain higher order correlation terms, models need to be developed to express them in terms of known or calculable variables.

2.1 Reynolds Stress Transport Equation Model

Turbulence models employing transport equations for $\overline{u_i u_j}$ are called second order closure smodels. Several closure schemes have been proposed for these equations. The well-tested one is that of Launder et al [21]. This model was applied to axisymmetric free shear flows by Launder and Morse [22]. The free-shear flow version of the transport equation for Reynolds stresses transport equations may be expressed as

$$\frac{D\overline{u_i u_j}}{Dt} = P_{ij} + \phi_{ij} - \varepsilon_{ij} + D_{ij} \tag{3}$$

Convection = Production + Pressure strain + Dissipation + Diffusion

The four terms on the right hand side represent the stress production, pressure-strain correlation, viscous dissipation and diffusive transport of $\overline{u_i u_j}$, respectively.

The pressure–strain correlation is approximated as:

$$\phi_{ij} = -c_1 \frac{\varepsilon}{k}\left(\overline{u_i u_j} - \frac{2}{3}\delta_{ij}k\right) - \alpha\left(P_{ij} - \frac{2}{3}\delta_{ij}P\right) - \beta\left(d_{ij} - \frac{2}{3}\delta_{ij}P\right) + \gamma k\left(\frac{\partial \overline{u}_i}{\partial x_j} + \frac{\partial \overline{u}_j}{\partial x_i}\right) \tag{4}$$

$$\varepsilon_{ij} = \frac{2}{3}\varepsilon\delta_{ij} \tag{5}$$

where

$$\varepsilon = \nu\overline{\left(\frac{\partial u_i}{\partial x_k}\right)^2}$$

$$P_{ij} = -\left[\overline{u_i u_k}\frac{\partial \overline{u}_j}{\partial x_k} + \overline{u_j u_k}\frac{\partial \overline{u}_i}{\partial x_k}\right] \tag{6}$$

$$d_{ij} = -\left(\overline{u_i u_k}\frac{\partial \overline{u}_k}{\partial x_j} + \overline{u_j u_k}\frac{\partial u_k}{\partial x_i}\right) \tag{7}$$

The coefficients α, β, and γ are related to a quantity c_2 by
$\alpha = (8+c_2)/11$; $\beta = (8c_2-2)/11$; $\gamma = (30c_2-2)/55$.
$P = P_{kk}/2$; $k = \overline{u_k u_k}/2$.

In [21], two models were adopted for the diffusive transport of stress, D_{ij}. The simpler one proposed by Daly and Harlow [23] was used for axisymmetric thin shear layers by Launder and Morse and it is:

$$D_{ij} = c_s \frac{\partial}{\partial x_k}\left(\frac{k}{\varepsilon}\overline{u_k u_l}\frac{\partial \overline{u_i u_j}}{\partial x_l}\right) \tag{8}$$

Closure of Launder et al model [21] is completed through the following equation for the turbulence dissipation rate, ε, of turbulence energy.

$$\frac{D\varepsilon}{Dt} = c_{\varepsilon 1}\frac{P\varepsilon}{k} - c_{\varepsilon 2}\frac{\varepsilon^2}{k} + c_\varepsilon \frac{\partial}{\partial x_k}\left(\frac{k}{\varepsilon}\overline{u_l u_k}\frac{\partial \varepsilon}{\partial x_l}\right) \tag{9}$$

The model contains six coefficients and their values are [22]:

c_1	c_2	c_s	$c_{\varepsilon 1}$	$c_{\varepsilon 2}$	c_ε
1.5	0.4	0.22	1.45	1.9	0.15

Convective transport and production terms are exact whereas the diffusion, pressure-strain, and viscous dissipation terms have been modeled. The diffusion fluxes of $\overline{u_i u_j}$ have been expressed by simple gradient diffusion models. The most important assumption concerns pressure-strain terms, since for shear stresses these are the main terms to balance the production of these quantities. The pressure strain model consists of two parts. The first one represents the interaction of fluctuating components only, and the second, the interaction of mean strain and fluctuating quantities: $\phi_{ij} = \phi_{ij}^{\,1} + \phi_{ij}^{\,2}$.

$$\phi^1{}_{ij} = -c_1\frac{\varepsilon}{k}\left(\overline{u_i u_j} - \frac{2}{3}\delta_{ij}k\right) \tag{10}$$

$$\phi^2{}_{ij} = -\alpha\left(P_{ij} - \frac{2}{3}\delta_{ij}P\right) - \beta\left(d_{ij} - \frac{2}{3}\delta_{ij}P\right) + \gamma k\left(\frac{\partial \overline{u}_i}{\partial x_j} + \frac{\partial \overline{u}_j}{\partial x_i}\right) \tag{11}$$

Several versions of pressure-strain model have been proposed to correctly predict the experimentally observed results. To account for the wall damping effects a wall correction must be introduced in the pressure-strain model. Launder et al [21] make the

empirical constants in the pressur-strain model a function of the relative distance from the wall, $l/y \propto k^{3/2}/(\varepsilon y)$. Because of the complexity and the large amount of computational effort involved, the model has not been widely used as one would like it to be.

2.2 Algebraic Stress Model

In Reynolds stress models, there are differential equations for each component of $\overline{u_i u_j}$ in addition to an ε equation. To reduce computational effort algebraic relations have been proposed by Rodi [24] for calculating the Reynolds stresses. This done by assuming that the net transport of $\overline{u_i u_j}$ is proportional to the net transport of k multiplied by the factor $\overline{u_i u_j}/k$.

Rodi uses a simpler model for pressure-strain relation than that presented in Eq. (4) and it is given by

$$\phi_{ij} = -c_1 \frac{\varepsilon}{k}\left(\overline{u_i u_j} - \frac{2}{3}\delta_{ij} k\right) - \alpha\left(P_{ij} - \frac{2}{3}\delta_{ij} P\right) \tag{12}$$

with $\alpha = 0.4$ and he writes the transport equation for turbulent energy, k as

$$\frac{Dk}{Dt} = c_s \underbrace{\frac{\partial}{\partial x_k}\left(\frac{k}{\varepsilon}\overline{u_k u_l}\frac{\partial k}{\partial x_l}\right)}_{D_k} - \underbrace{\overline{u_k u_l}\frac{\partial \overline{u_i}}{\partial x_k}}_{P=P_{ii}/2} \tag{13}$$

As mentioned above, to obtain an algebraic expression for $\overline{u_i u_j}$, the following approximation is employed:

$$\frac{D\overline{u_i u_j}}{Dt} - D_{ij} = \frac{\overline{u_i u_j}}{k}\left(\frac{Dk}{Dt} - D_k\right) = \frac{\overline{u_i u_j}}{k}(P - \varepsilon) \tag{14}$$

where D_{ij} is defined in Eq. (8), D_k and P in Eq. (13). Incorporation of Eq. (14) into the $\overline{u_i u_j}$ equation (3) yields the desired algebraic expression for $\overline{u_i u_j}$:

$$\overline{u_i u_j} = k\left[\frac{2}{3}\delta_{ij} + \frac{1-\alpha}{c_1}\frac{P_{ij}/\varepsilon - \frac{2}{3}\delta_{ij} P/\varepsilon}{1 + \frac{1}{c_1}\left(\frac{P}{\varepsilon} - 1\right)}\right] \tag{15}$$

Now we have a set of algebraic expressions for the stresses $\overline{u_i u_j}$, in terms of the mean strain rate, turbulent kinetic energy k, and its dissipation rate ε, and the stresses themselves. As in Launder et al model [21], closure is completed by an equation for the dissipation rate of turbulence energy, ε.

The algebraic stress model provides a mechanism by which anisotropic turbulence distribution can be computed without the large amount of computational effort required for the Reynolds stress transport equation model discussed above. All the effects that enter the transport equations for $\overline{u_i u_j}$ through the source terms for example, body force effects (buoyancy, rotation, and streamline curvature), non-isotropic strain field and wall damping influence can be incorporated into algebraic stress models. Algebraic stress models therefore also simulate many of the flow phenomena that were described successfully by Reynolds stress transport equation models.

2.3 k-ε Model

The k-ε model is the most often used model in present day engineering computations. The model was developed by Launder and Spalding [25,26] and Hanjalic and Launder [27]. In this model closure is achieved by relating the Reynolds stress to the mean strain rate through the Boussinesq approximation

$$-\rho\overline{u_i u_j} = \mu_t\left(\frac{\partial \bar{u}_i}{\partial x_j}+\frac{\partial \bar{u}_j}{\partial x_i}\right)-\frac{2}{3}\delta_{ij}\rho k \tag{16}$$

The effective turbulent viscosity, μ_t is defined in terms of a characteristic length and velocity. If the length scale is taken as the turbulent length scale, $k^{3/2}/\varepsilon$, and the velocity scale is approximated as $\sqrt{k}$, then μ_t can be expressed as

$$\mu_t = c_\mu \rho k^2/\varepsilon \tag{17}$$

c_μ is a constant. The individual $\overline{u_i u_j}$ is related to the single velocity scale $\sqrt{k}$. For isotropic turbulence $\overline{u_i u_j}$ =2/3 $\delta_{ij}k$. In k-ε model one solves two separate modeled transport equations, one for turbulent kinetic energy and the other for its dissipation rate. The modeled equations for k and ε as described in Reference 26 are:

(a) Kinetic energy equation

$$\frac{Dk}{Dt}=\frac{1}{\rho}\frac{\partial}{\partial x_k}\left[\frac{\mu_t}{\sigma_k}\frac{\partial k}{\partial x_k}\right]+\frac{\mu_t}{\rho}\left(\frac{\partial \bar{u}_i}{\partial x_k}+\frac{\partial \bar{u}_k}{\partial x_i}\right)\frac{\partial \bar{u}_i}{\partial x_k}-\varepsilon \tag{18}$$

(b) Kinetic energy dissipation rate equation

$$\frac{D\varepsilon}{Dt} = \frac{1}{\rho}\frac{\partial}{\partial x_k}\left[\frac{\mu_t}{\sigma_\varepsilon}\frac{\partial \varepsilon}{\partial x_k}\right] + \frac{c_{\varepsilon 1}\mu_t}{\rho}\frac{\varepsilon}{k}\left(\frac{\partial \overline{u}_i}{\partial x_k} + \frac{\partial \overline{u}_k}{\partial x_i}\right)\frac{\partial \overline{u}_i}{\partial x_k} - c_{\varepsilon 2}\frac{\varepsilon^2}{k} \tag{19}$$

The constants assume the approximate values of $c_\mu = 0.09$, $c_{\varepsilon 1} = 1.44$, $c_{\varepsilon 2} = 1.92$, $\sigma_k = 1.0$, and $\sigma_\varepsilon = 1.3$. These constants were obtained by comparison of model predictions with the experimental data on equilibrium boundary layers and decay of isotropic turbulence.

III. MODIFICATIONS TO k-ε MODEL

The standard k-ε model has been modified to account for observed discrepancies between the model prediction and the experimental results. Here we consider first two such modifications relevant for the computation of jet flows to account for the spreading rate of circular jets and the spreading rate of high-speed jets. Then we discuss an anisotropic k-ε model, low Reynolds number and near-wall models, and multiple-scale models.

3.1 Vortex stretching dependent dissipation rate

It was found early on that while the standard k-ε model predicts the plane jet flow correctly, it overestimates the spreading rate of circular jets. Pope [28] suggested that the stretching of vortex tubes by the mean flow has significant influence on the process of turbulence scale reduction. In axisymmetric jets, as the jet spreads rings of vorticity are stretched. This causes the effective viscosity and hence the spreading rate to be lower in the circular jet. Pope incorporated this aspect in the standard k-ε model by modifying the dissipation rate, ε, equation. The modified form of the dissipation equation proposed by him is:

$$\frac{D\varepsilon}{Dt} = \frac{1}{\rho}\frac{\partial}{\partial x_k}\left[\frac{\mu_t}{\sigma_\varepsilon}\frac{\partial \varepsilon}{\partial x_k}\right] + \frac{c_{\varepsilon 1}\mu_t}{\rho}\frac{\varepsilon}{k}\left(\frac{\partial \overline{u}_i}{\partial x_k} + \frac{\partial \overline{u}_k}{\partial x_i}\right)\frac{\partial \overline{u}_i}{\partial x_k} - c_{\varepsilon 2}\frac{\varepsilon^2}{k} + c_{\varepsilon 3}\chi \tag{20}$$

Where $\chi = \omega_{ij}\omega_{jk}s_{ij}$

$$s_{ij} = \frac{1}{2}\frac{k}{\varepsilon}\left(\frac{\partial \overline{u}_i}{\partial x_j} + \frac{\partial \overline{u}_j}{\partial x_i}\right) \tag{21}$$

$$\omega_{ij} = \frac{1}{2}\frac{k}{e}\left(\frac{\partial \overline{u}_i}{\partial x_j} - \frac{\partial \overline{u}_j}{\partial x_i}\right) \tag{22}$$

and $c_{\varepsilon 3} = 0.79$.

3.2 Compressibility Correction

The standard k-ε model when used to predict the development of high-speed shear layers and jets, it was found that the growth rate did not compare well with the measurements. In these flows, the experiments showed that the growth rate of high-speed shear layers reduces with increase in convective Mach number [29]. The growth rate of shear layers is dependent on the growth rate of instability waves at these speeds. At high speeds, the reduction in the instability wave growth rate reduces turbulent mixing. Sarkar et al [30], Sarkar and Lashhmanan [31], and Sarkar [32], developed an addtitonal factor to be added to the standard k-ε model to account for the compressibility effects. The form of the additional factor was found by an asymptotic analysis of the compressible Navier-Stokes equations. The suggested modification is

$$\varepsilon = \varepsilon_s(1+\alpha M_t^2) \tag{23}$$

where $M_t^2 = 2k/(\gamma R_{gT})$ and α is a constant set equal to 1.0 and R_g is the gas constant.

The factor $\varepsilon = \varepsilon_s(1+\alpha M_t^2)$ corresponds to the contribution due to the incompressible and compressible dissipation rates, ε_s referring to the standard value and M_t is the turbulent Mach number. This term is added to the turbulent kinetic energy equation of the standard k-ε model. The equation now reads as

$$\frac{Dk}{Dt} = \frac{1}{\rho}\frac{\partial}{\partial x_k}\left[\frac{\mu_t}{\sigma_k}\frac{\partial k}{\partial x_k}\right] + \frac{\mu_t}{\rho}\left(\frac{\partial \bar{u}_i}{\partial x_k} + \frac{\partial \bar{u}_k}{\partial x_i}\right) - \varepsilon(1+\alpha M_t^2) \tag{24}$$

3.3 Anisotropic k-ε Model

The standard k-ε model assumes an isotropic eddy viscosity relationship for the Reynods stress tensor. Reynolds stress models discussed above can predict the observed anisotropy in normal stresses. Anisotropic k-ε models based on anisotropic eddy diffusivitites have been proposed [33-38]. The anisotropic model proposed by Myong and Kasagi [35], is valid up to the wall. In this model, the deviations from isotropic Reynolds stresses are given by a function of nonlinear quadratic terms of mean velocity gradients and that of anisotropic diffusion terms of turbulent kinetic energy. The normal Reynolds stresses are algebraically calculated. The expression for Reynolds stress is given as:

$$\frac{Dk}{Dt} = \frac{\partial}{\partial x_j}(\nu + \nu_t/\sigma_k)\frac{\partial k}{\partial x_j} - \overline{u_i u_j}\frac{\partial \bar{u}}{\partial x_j} - \varepsilon \tag{25}$$

$$\frac{D\varepsilon}{Dt} = \frac{\partial}{\partial x_j}\left[(\nu + \frac{\nu_t}{\sigma_\varepsilon})\frac{\partial \varepsilon}{\partial x_j}\right] - c_{\varepsilon 1}\frac{\varepsilon}{k}\overline{u_i u_j}\frac{\partial \bar{u}_i}{\partial x_j} - c_{\varepsilon 2} f_2 \frac{\varepsilon^2}{k} \tag{26}$$

Where

$$\overline{u_i u_j} = \frac{2}{3}k\delta_{ij} - \nu_t\left[\frac{\partial \bar{u}_i}{\partial x_j} + \frac{\partial \bar{u}_j}{\partial x_i}\right] + \frac{k}{\varepsilon}\nu_t \sum_{\beta=1}^{3} c_\beta\left(S_{\beta ij} - \frac{1}{3}S_{\beta\alpha\alpha}\delta_{ij}\right) + \sum_n \frac{2}{3}\nu\frac{k}{\varepsilon}W\left(\frac{\partial\sqrt{k}}{\partial x_n}\right)^2\delta_{ij} \tag{27}$$

$$S_{1ij} = \frac{\partial \bar{u}_i}{\partial x_k}\frac{\partial \bar{u}_j}{\partial x_k}, \quad S_{2ij} = \frac{1}{2}\left(\frac{\partial \bar{u}_k}{\partial x_i}\frac{\partial \bar{u}_j}{\partial x_k} + \frac{\partial \bar{u}_k}{\partial x_j}\frac{\partial \bar{u}_i}{\partial x_k}\right) \quad S_{3ij} = \frac{\partial \bar{u}_k}{\partial x_i}\frac{\partial \bar{u}_k}{\partial x_j}, \tag{28}$$

$$\nu_t = c_\mu \sqrt{k} L = c_\mu f_\mu \frac{k^2}{\varepsilon} \tag{29}$$

$$f_\mu = (1 - \frac{3.45}{\sqrt{R_t}})\left[1 - \exp(-\frac{y^+}{70})\right] \tag{30}$$

$$f_2 = (1 - \frac{2}{9}\exp[-(\frac{R_t}{6})^2])[1 - \exp(-\frac{y^+}{5})]^2 \tag{31}$$

$$W = -1.5 - 0.75(\delta_{in}\delta_{in} + \delta_{jn}\delta_{jn}) + 2(\delta_{im}\delta_{im} + \delta_{jm}\delta_{jm}) + \delta_{in}\delta_{jn}\delta_{ij} + \delta_{im}\delta_{jm}\delta_{ij} \tag{32}$$

$R_t = k^2/\nu\varepsilon$; $\delta_k = 1.4$, $\delta_\varepsilon = 1.3$, $c_{\varepsilon 1} = 1.4$, $c_{\varepsilon 2} = 1.8$, and $c_\mu = 0.09$.

(The indices n and m denote the wall normal and streamwise coordinates respectively).

The mean velocity, the turbulent kinetic energy and its dissipation rate are not influenced by the normal stress anisotropy. The transport equations to be solved are similar to those of isotropic k-ε model.

Myong and Kasagi [35] showed that their anisotropic model predicts correctly the dependence of each normal component of Reynods stress correctly, u α y, v α y^2, and w α y [Fig. 1]. For the flow over a flat plate, the model predicts the wall-limiting behavior that is in good agreement with the data [Fig. 2]. The predicted Reynolds stress

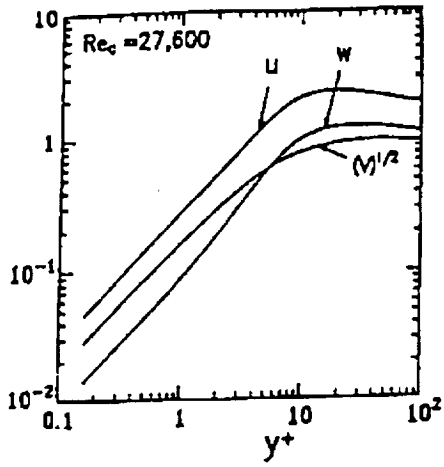

Fig. 1 Wall-limiting behavior of three normal Reynolds stresses -- after Myong and Kasagi [35]

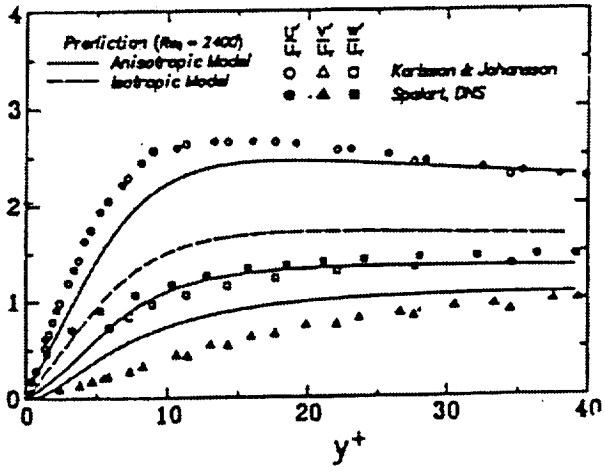

Fig.2 Distributions of normal Reynolds stresses in a turbulent boundary layer – after Myong and Kasagi [35]

components in the entire region were also found to agree fairly well with the experimental results.

3.4 Low Reynolds Number and Near Wall k-ε Model

Jones and Launder [36], extended the k-ε model to model low Reynolds number flows so that the turbulence model equation can be valid throughout the laminar, transition, and fully turbulent regions. In this version of the model k and ε are determined from the following equations:

$$\frac{Dk}{Dt} = \frac{1}{\rho}\frac{\partial}{\partial x_k}\left[\left(\mu + \frac{\mu_t}{\sigma_k}\right)\frac{\partial k}{\partial x_k}\right] + \frac{\mu_t}{\rho}\left(\frac{\partial \bar{u}_i}{\partial x_k} + \frac{\partial \bar{u}_k}{\partial x_i}\right)\frac{\partial \bar{u}_i}{\partial x_k} - 2\nu\left(\frac{\partial k^{1/2}}{\partial x_j}\right)^2 - \varepsilon \tag{33}$$

$$\frac{D\varepsilon}{Dt} = \frac{1}{\rho}\frac{\partial}{\partial x_k}\left[\left(\mu + \frac{\mu_t}{\sigma_\varepsilon}\right)\frac{\partial \varepsilon}{\partial x_k}\right] + \frac{c_{\varepsilon 1}\mu_t}{\rho}\frac{\varepsilon}{k}\left(\frac{\partial \bar{u}_i}{\partial x_k} + \frac{\partial \bar{u}_k}{\partial x_i}\right)\frac{\partial \bar{u}_i}{\partial x_k} - c_{\varepsilon 2}\frac{\varepsilon^2}{k} - 2.0\frac{\nu\mu_t}{\rho}\left(\frac{\partial^2 \bar{u}_i}{\partial x_i \partial x_i}\right) \tag{34}$$

μ_t is the turbulent viscosity defined, for the standard k-ε model, in Eq. (17). In this model, c_μ and $c_{\varepsilon 2}$ vary with turbulence Reynolds number, R_t.

$$R_t = \rho k^2/\mu\varepsilon \tag{35}$$

$$c_\mu = c_{\mu s}\exp[-2.5/(1+R_t/50)] \tag{36}$$

$$c_{\varepsilon 2} = c_{\varepsilon 2 s}\,[1-0.3\exp(-R_t^2)] \tag{37}$$

Subscript s refers to the standard model values. We note here, that the laminar diffusive transport becomes of increasing importance as the wall is approached and the extra destruction terms included are of some significance in the viscous and transitional regions. The term,

$$2.0\frac{\nu\mu_t}{\rho}\left(\frac{\partial^2 \bar{u}_i}{\partial x_i \partial x_i}\right)$$

in the ε equation produces satisfactory variation of k with distance from the wall. In the computations ε is set to zero at the wall and an extra term,

$$-2\nu\left(\frac{\partial k^{1/2}}{\partial x_j}\right)^2$$

is introduced to the k equation. This extra term is exactly equal to the energy dissipation rate in the neighborhood of the wall.

Turbulence models for near wall and low Reynolds number flows were reviewed by Patel et al [37]. Eight different models (all based on k-ε model except one) were considered and their performance in predicting turbulent boundary layers with and without pressure gradient (favorable/adverse) was examined. The model of Launder and Sharma [38] and that of Chien [39], both based on Jones and Launder model described above appear to perform well in majority of the test cases studied by Patel et al [37].

The model of Chien [39] is claimed to perform better than that of Jones and Launder is briefly described here. Though the model is based on Jones and Launder model, the presence of solid wall is handled differently. An additional term, representing the finite dissipation rate at the wall, is added to balance the molecular diffusion term. The dissipation term in the kinetic energy equation is given by $\varepsilon + (2\nu k/y^2)$ for finite values of y, distance from the wall. The turbulent kinetic energy equation takes the form

$$\frac{Dk}{Dt} = \frac{\partial}{\partial y}\left[(\nu + \nu_t)\frac{\partial k}{\partial y}\right] + \nu_t\left(\frac{\partial u}{\partial y}\right)^2 - \varepsilon - \frac{2\nu k}{y^2} \tag{38}$$

The term

$$-\frac{2\nu k}{y^2}$$

is the term added to produce correct behavior of turbulent energy k in the near wall region. ν is the kinematic viscosity. The turbulent viscosity ν_t is modified to reflect the wall damping effect.

$$\nu_t = c_\mu \frac{k^2}{\varepsilon}\left(1 - \exp(-c_3 u^* y/\nu)\right) \tag{39}$$

c_3 is a constant. u^* is the friction velocity. The turbulent dissipation rate equation suggested by Chien reads as

$$\frac{D\varepsilon}{Dt} = \frac{\partial}{\partial y}\left[(\nu + \frac{\nu_t}{\sigma_\varepsilon})\frac{\partial \varepsilon}{\partial y}\right] + c_{\varepsilon 1}\frac{\varepsilon}{k}\nu_t\left(\frac{\partial u}{\partial y}\right)^2 - \frac{\varepsilon}{k}\left[c_{\varepsilon 2} f\varepsilon + \frac{2\nu k \exp(-c_4 u^* y/\nu)}{y^2}\right] \tag{40}$$

where $f = 1\text{-}0.222\ \exp[-(R_t/6)^2]$, c_4 is a constant. $c_3 = 0.0115$ and $c_4 = 0.5$ were used by Chien.

3.5 Multiple-Scale Model

The turbulence models discussed above are based on the assumption that in all flow situations turbulence has a spectrum of universal form which can be characterized by the scale of the energy containing range. Difficulties arise when the spectrum is not an equilibrium one or when the flow exhibits distinctly different ranges of scales. A two-scales model was proposed by Hanjalic et al [40] . They split the spectrum into a large scale part and a small scale part with different time scales for energy transfer into the large scale part and transfer from large scale to small scale part.

The turbulence spectrum consists of independent production, inertial, and dissipation ranges. K_1 denotes the wave number above which a significant mean strain production occurs while K_2 is the largest wave number at which viscous dissipation of turbulence is unimportant (Fig. 3). Energy leaves the first region (production) at a rate ε_p and enters the high wave number or dissipation region at a rate ε_t. Between the two regions, occupying the intermediate range of wave numbers is the transfer region, across which a representative spectral energy transfer rate ε_T is assumed. This simplified energy spectrum is the basis of the model of Hanjalic et al. The total turbulence energy k is assumed to be divided between production range k_p and the transfer range k_T. At high Reynolds numbers there is negligible kinetic energy in the dissipation range. The transport equations for k_p, k_T, ε_p, and ε_T are formulated. Thus there are two k and two ε equations in this model and two sets of constants which are determined from experiments.

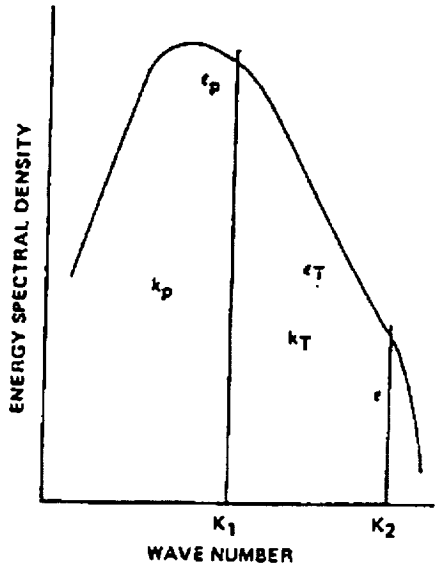

Fig. 3 The spectral division for multiple scale model – after Hanjalic et al [40]

Modified versions of the above two-scale model have been formulated by Kim & Chen [41] and Chen [42]. In the model used by Duncan et al [43], the model coefficients were made dynamically dependent on the partitioning of the energy spectrum. Ko and Rhode [44] developed a new multi-scale k-ε turbulence model, which incorporated a new way of evaluating source/sink coefficient functions. Though these models are attractive from a theoretical viewpoint, their use to flows of engineering interest is hampered by the number of constants needed to be calibrated with these models.

Next, the application of the turbulence models to the prediction of jet nose shall be discussed.

IV. TURBULENCE MODELS AS APPLIED TO JET NOISE PREDICTION

4.1 k-ε Model Computations for Jet Noise Prediction

The quadrupole source term (unsteady Reynolds stress) that appears in Lighthill's equation has to be evaluated to compute the jet noise. In the absence of detailed time dependent flow information, one uses the mean flow information from a simplified turbulent flow model such as that of Reichardt's[45]. Suggestions were made that with the advances in computational fluid dynamics (CFD), the source terms can be computed more accurately from the solution of Reynolds averaged Navier-Stokes equations using a k-ε model[46]. Khavaran et al [6] were the first to carry out such a source computation and use the source characteristics for the computation of jet noise. They considered a convergent-divergent nozzle geometry. The flow solution was obtained using an axisymmetric version of PARC code [47] with Chiens's k-ε model [39]. They showed good agreements of the CFD results with the data. The computed turbulence intensity contours in the flow field are shown in Fig. 4. Comparisons of the computed turbulence intensities with the data and the Reichardt's solution are shown in Fig. 5.

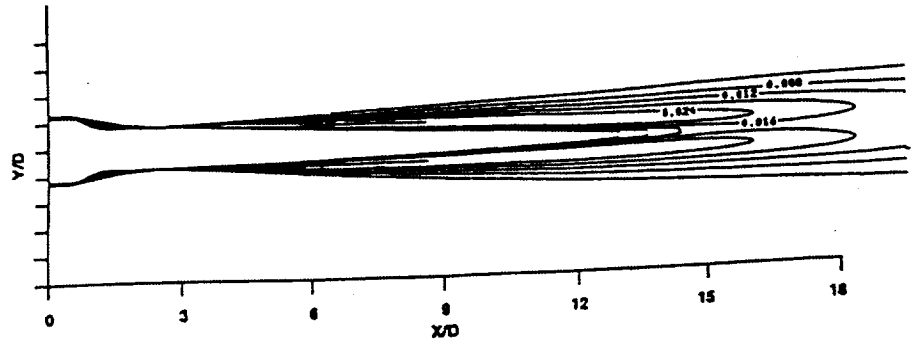

Fig. 4 Tubulent intensity contours in a round jet – after Khavaran et al [6]

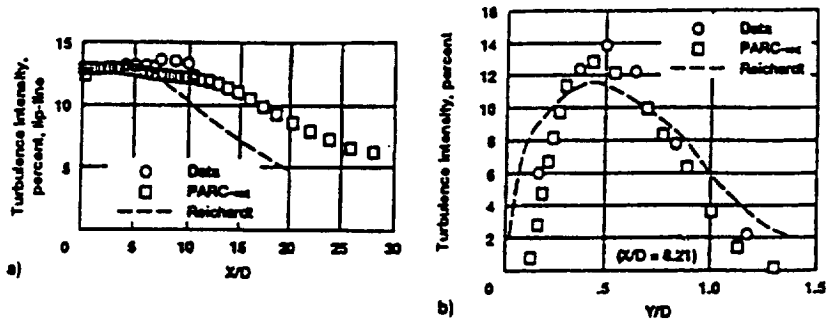

Fig. 5 Comparison of predicted and experimental turbulent intensities
(a) Lip-line and (b) X/D = 8.21 – after Khavarn et al [6]

The time averaged flow information is used to compute the sound field: The noise source strength in a turbulent flow is characterized by a two-point time delayed fourth order velocity correlation tensor. The fourth order correlation is expressed as a linear combination of second order correlations. Then, the two point velocity correlations are written in terms of separable space/time factors as suggested by Ribner [48],

$$\overline{u_i u'_j} = R_{ij}(\xi)g(\tau) \tag{41}$$

The space factor $R_{ij}(\xi)$ is expressed as a function of turbulence intensity and the longitudinal macroscale of turbulence. The time correlation is expressed in terms of the characteristic time delay, τ_o, which is proportional to the inverse of mean shear and is related to turbulence kinetic energy k ($k = \overline{u_i u_i}/2$) and its dissipation rate ε as $\tau_o = k/\varepsilon$. Thus, the noise source strengths can be expressed in terms of length and time scales extracted from time averaged solutions. The corresponding spectrum can then be evaluated by a using a Fourier transform on the time delay of correlation.

Khavaran et al evaluated the contribution to self noise for various source strength components using Ribner's formulation [48]. The contribution to the acoustic pressure, $p(R,\theta,\Omega)$, due to each quadrupole source may be expressed as

$$P^2(R,\theta,\Omega) \quad \propto \quad k^{7/2}(\Omega\tau_o)^4 \exp\left[-\frac{1}{8}(\Omega\tau_o)^2\right] \tag{42}$$

where R is the radius, θ is the angle with respect to jet axis and Ω the source frequency. It is seen that for accurate prediction of acoustic pressure, the turbulent kinetic energy and its dissipation rate ε need to be computed accurately by the flow solution ($\tau_o = k/\varepsilon$). Further details of the noise computation can be found in [6]. Comparisons of the overall sound pressure level directivity show good agreement with the data and the results of Reichardt method (Fig. 6). The spectral components of noise, based on the one-third octave band, are shown in Fig. 7.

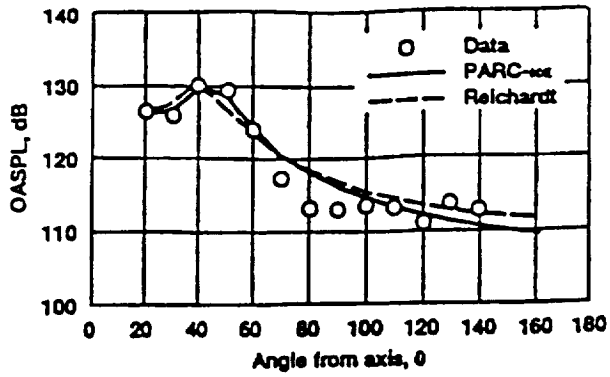

Fig. 6 Comparison of overall sound pressure level directivity with data on a 40-ft radius – after Khavaran et al [6].

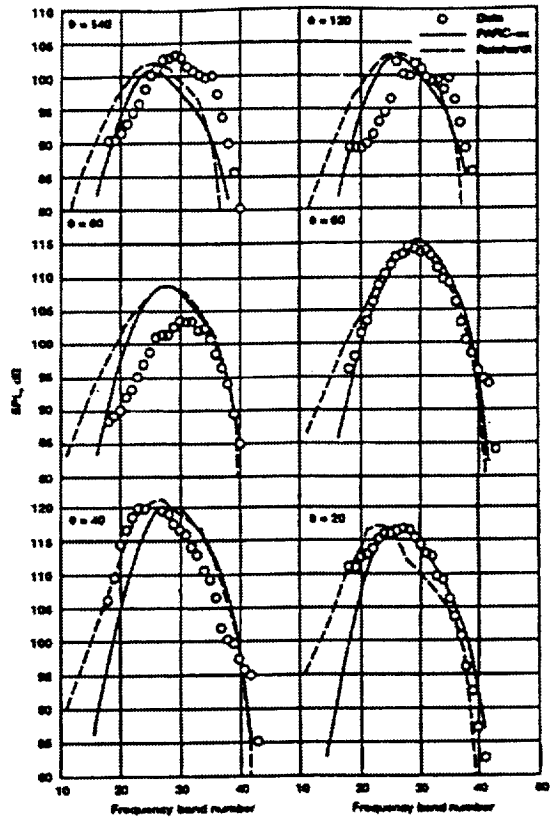

Fig. 7 Comparison of the spectral components of noise with data based on one-third octave center frequency (band number 11 corres›onds to 50 Hz). – after khavaran et al [6]

Bailly et al [7,8] used a similar approach and computed the jet noise using the source strength obtained from a CFD solution using k-ε model. They computed far-field levels using Ribner's model and also that of Goldstein and Rosenbaum [49] who modified the Ribner model by introducing an anisotropic description of turbulent field. They found that Goldstein and Rosenbaum model produced better agreement with the far-field sound pressure data.

For supersonic jets, Bailly et al used Ffowcs-Williams and Maidanic [50] formulation of Lighthill source term to account for Mach wave radiation which is one of the main noise source in supersonic jets. They applied this model when the local convective Mach number is supersonic. Using a combination of Goldstein and Rosenbaum model and Ffowics-Williams and Maidanic model, they were able to compute the far-field acoustic pressure as a function of jet Mach number, from low subsonic to high supersonic jets. The computed far-field levels were found to be in good agreement with the data (Fig. 8).

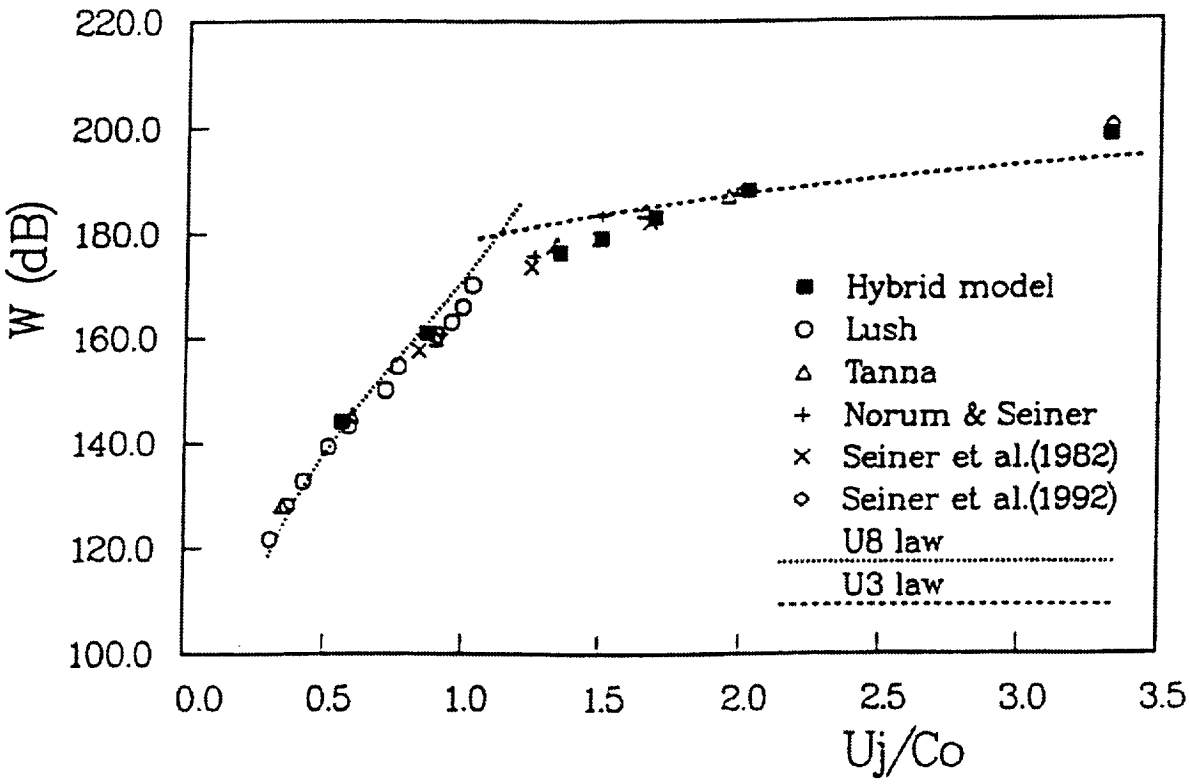

Fig. 8 Total acoustic power as a function of jet Mach number: comparison Of hybrid noise model to experimental data – after Bailly et al [7]

However, the description of the two-point velocity correlation needs to be further examined to improve the source definition and better establish the proportionality factors that arise from the use of time averaged quantities.

Measured turbulence intensities in nozzle flows show considerable anisotropy among turbulence intensity components. Longitudinal component (u_1) is significantly different from the transverse components (u_2 and u_3). The transverse components (u_2 and u_3) are nearly equal. To account for the observed anisotropy Khavaran and Krejsa [9] proposed the use of an axisymmetric turbulence model for jet noise computation. However, since the CFD solutions were obtained with a k-ε model (isotropic turbulence assumed) they investigate the influence of anisotropy by varying the ratio of transverse to longitudinal length scales, Δ_l, and the ratio of intensities, $\Delta_u = u_2^2/u_1^2$. They demonstrated the effects of the parameters on the noise directivity of a splitter nozzle flow. The predicted noise directivity shows good agreement with the data when the parameter $\Delta_l = 0.5$ and $\Delta_u = 0.6$ (Fig. 9). The effects of anisotropy parameters are summarized in Fig. 10. An increase in anisotropy tends to increase the sound pressure level. The use of axisymmetric turbulence model for noise computation would improve the noise predictive capability of jets of practical interest.

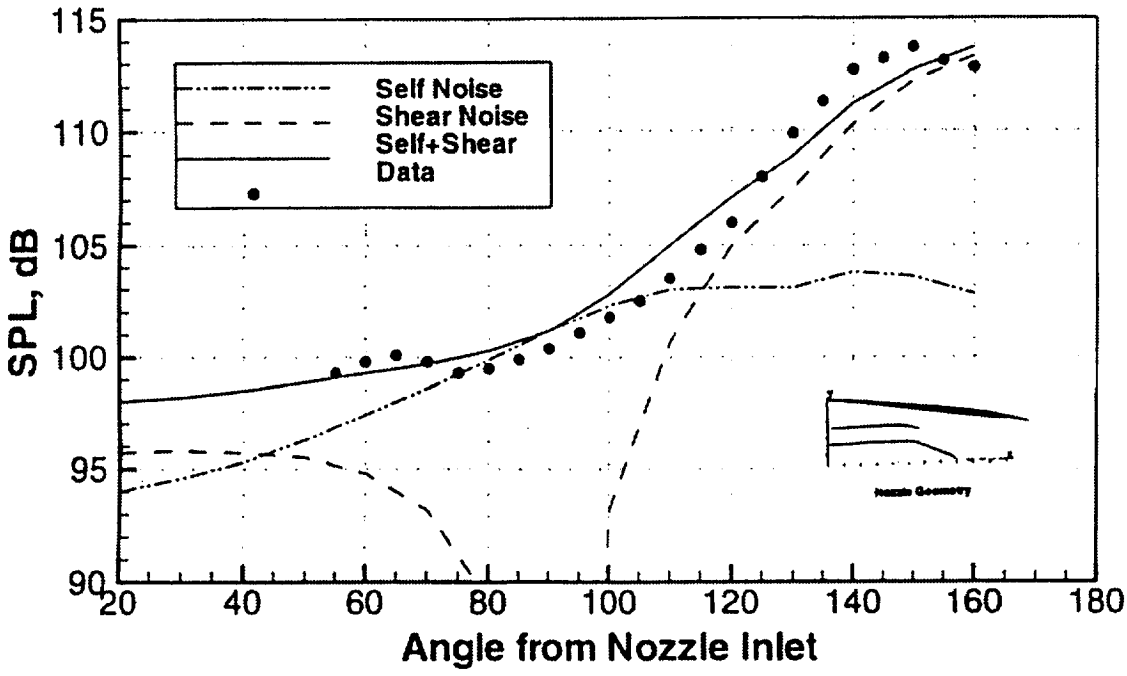

Fig. 9 Predicted sound pressure level directivity for the splitter nozle on a 50 ft arc. Anisotropy parameters are: $\Delta = 0.50$ and $u_2^2/u_1^2 = 0.60$. – after Khavarn and Krejsa [9].

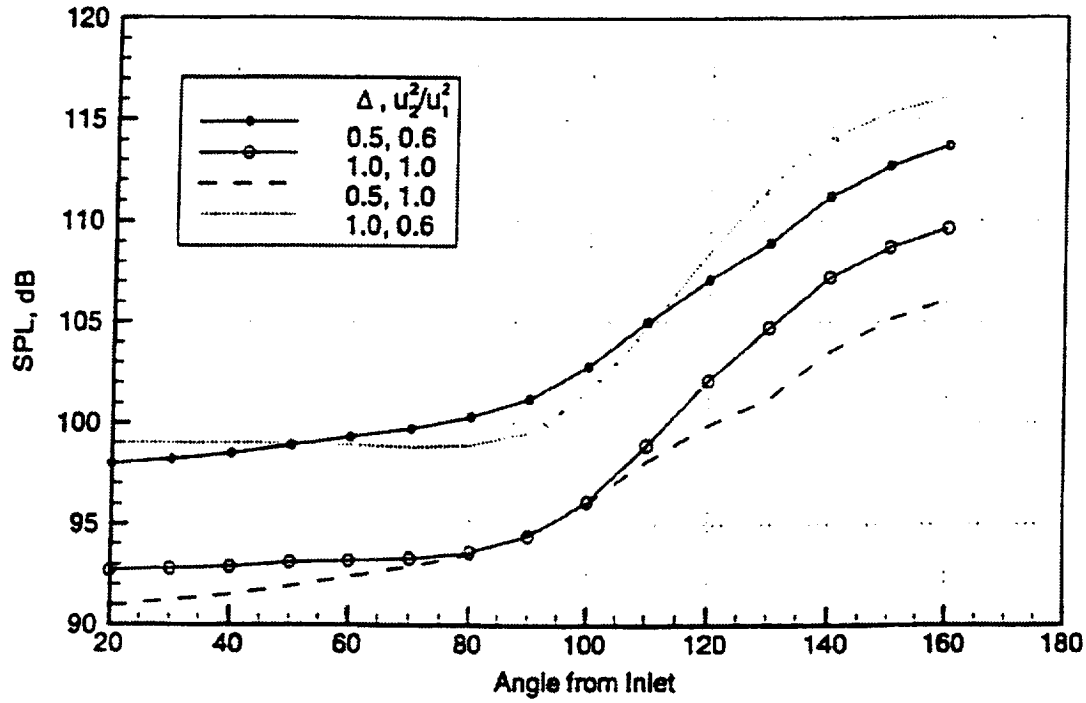

Fig. 10 Sound pressure level directivity vs. non-isotropy parameters Δ and u_2^2/u_1^2. – after khavaran and Krejsa [9]

Since, distributions of u_1^2 and u_2^2 are needed for the prediction of jet noise, ways to obtain these components should be explored. The possibilities exist to use the Reynolds stress transport equation model or the algebraic stress model (ASM) described in section 2.

4.2 Other k-ε Model Predictions

Here, some other applications of turbulence models to jet flow predictions that produce reasonable solutions that may be used for jet noise prediction are discussed.

Numerous k-ε model predictions have been carried out for jet flows. But these predictions were mainly intended to study the flow field characteristics and they have not been used for the purpose of noise prediction. Some of them are reviewed here, as they hold promise for noise predictions.

One of the most exhaustive applications of k-ε model for jet flows encompassing subsonic, supersonic, cold and hot jet flows is that of Thies and Tam [51]. The jet Mach number varied from 0.4 to 2.2 and the ratio of jet reservoir temperature to ambient temperature varied from 1.0 (cold jet) to 4.0. They demonstrated that if the original constants of the k-ε model are replaced by a new set of constants (established

empirically), the calculated jet mean velocity profiles agreed with the data for a wide range of jet flows. They included the correction term for vortex stretching due to Pope [28] and compressibility correction due to Sarkar [32], but with new empirically established constants. Their choices of model constants are:

c_μ	$c_{\varepsilon 1}$	$c_{\varepsilon 2}$	$c_{\varepsilon 3}$	σ_k	σ_ε	α
0.0874	1.4	2.02	0.822	0.324	0.377	0.518

Note that the factor associated with the vortex stretching term, $c_{\varepsilon 3}$, and the factor, α, associated with the compressibility correction term are also modified. The parabolized equations, in the Favre-averaged form, are solved using an accurate dispersion-relation-preserving (DRP) numerical scheme. In all the cases the computation started from the nozzle exit, with initial conditions derived analytically or from the data. The predicted mean velocities agreed well with the data as shown in Fig. 11 for heated jets.

Dash et al [52-54] in a series of papers have explored different formulations of k-ε model and its various combinations for jet flow predictions. A k-ε model with modified compressible dissipation factor (due to Sarkar [32] and Zeman [55]) and with Pope correction factor was found to yield reasonably good predictions over a range of jet flow conditions. They expressed the compressible dissipation as

$$\varepsilon_c = \varepsilon_s \left[\alpha \overline{M}_t^2 + \beta \overline{M}_t^4 \right] \tag{43}$$

where $\alpha = 1$ (same as Sarkar) and $\overline{M_t} = M_t - \lambda$.

$\lambda = 0.1$ (same as Zeman)

and $\beta = 60$, to fit LaRC data best.

An example of their predictions of centerline velocity (Fig. 12) and temperature (Fig. 13) for different jet exit temperatures of Seiner's [56] jet are shown. The trends are predicted reasonably well.

The use of compressible dissipation factor for supersonic jet flow predictions was also studied by Balakrishnan et al [57]. They found that with the compressible dissipation correction the reduced spreading rate of supersonic jets was successfully predicted (Fig. 14). The prediction of pressure distribution in an under-expanded jet with and without compressibility correction is shown in Fig. 15. The improvements observed due to compressibility correction factor in predicting turbulence intensities in an under expanded jet are shown in Fig. 16. for two numerical algorithms.

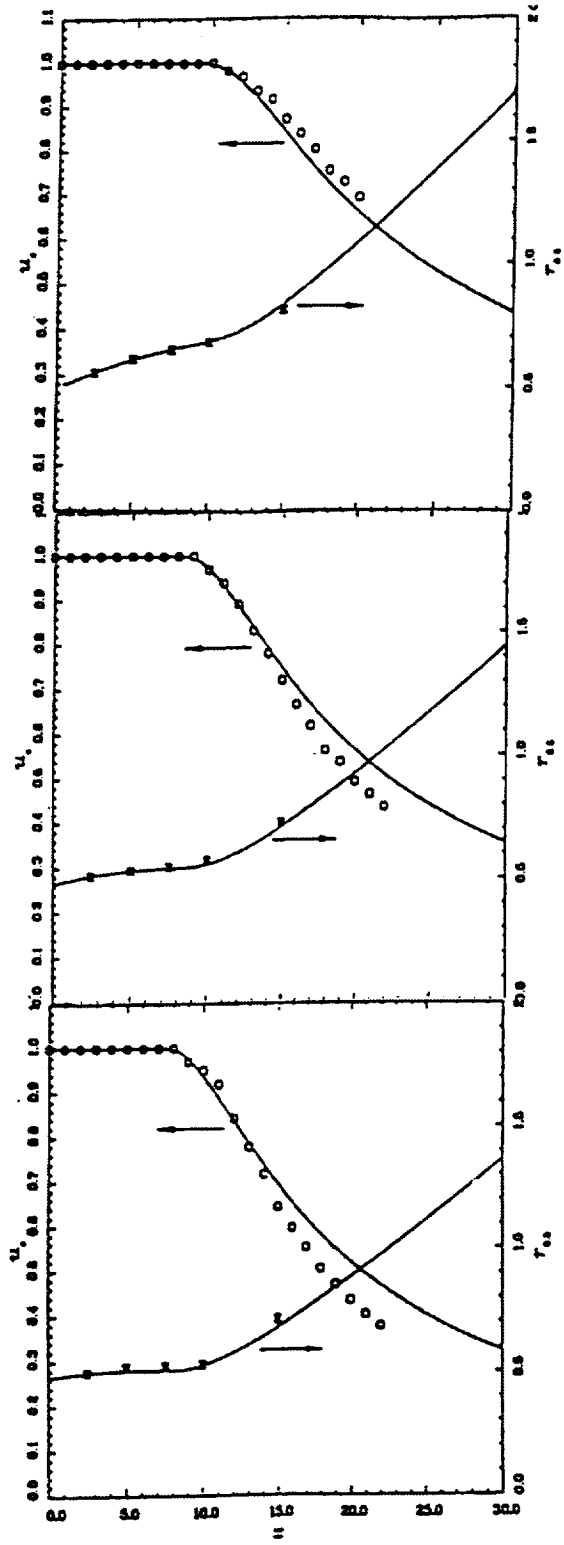

Fig. 11 Comparisons of computed and measured center line velocity and half-velocity point distributions for Seiner et al's [53] Mach 2.0, axisymmetric jet: o, asured centerline velocity and II, measured half-velocity point. – after Thies and Tam [51]

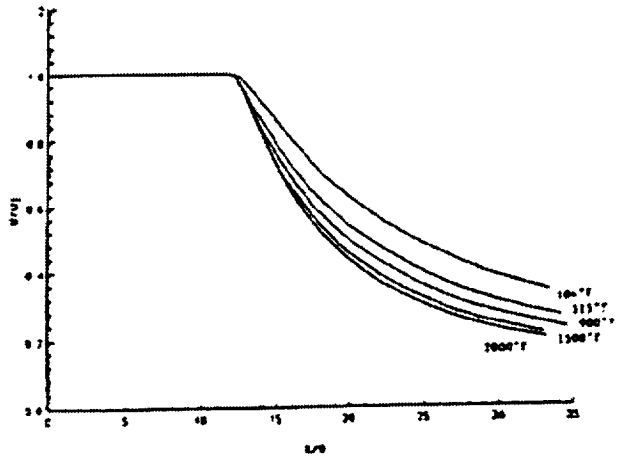

Fig. 12 Axis velocity decay of the Seiner Mach 2 jet cases into still air using the jet modified kεCD model with the Pope centerline correction. – after Dash et al. [52]

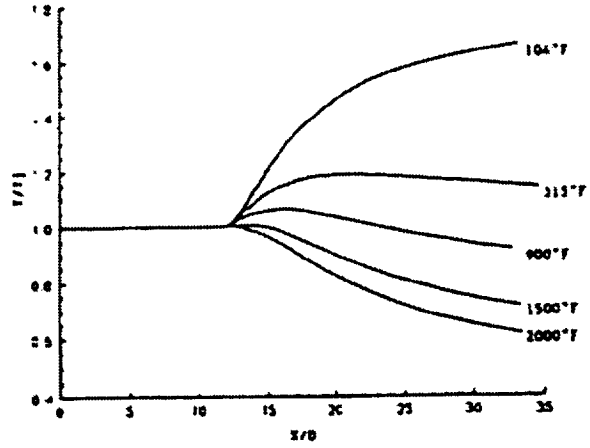

Fig. 13 Axis temperature decay of the Seiner Mach 2 jet cases into still air using the jet Modified kεCD model with the Pope centerline correction. – after Dash et al [52]

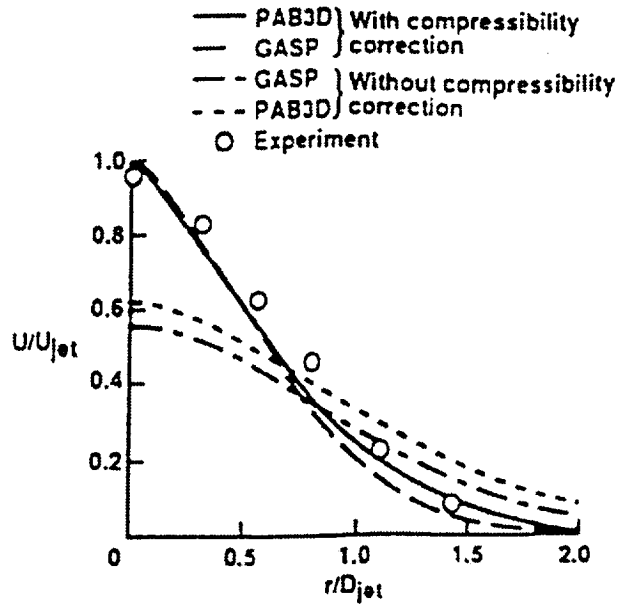

Fig. 14 Velocity profile at X/D = 13.5 for a supersonic jet. – after Balakrishnan and Abdol-Hamid [57].

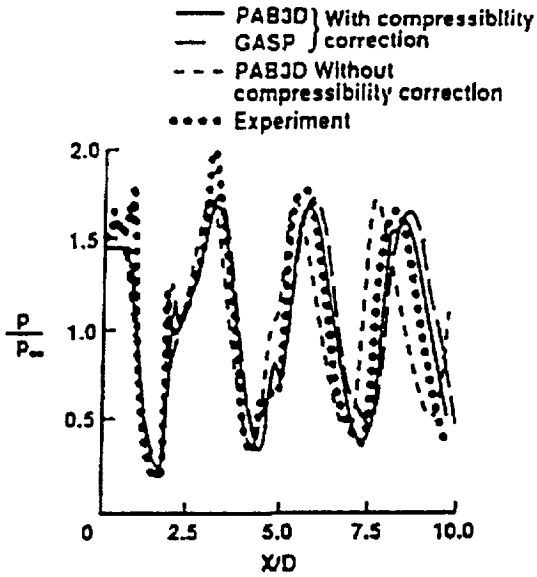

Fig. 15 Centerline pressure distribution for an underexpanded supersonic jet. – after Balakrishnan and Abdol-Hamid [57]

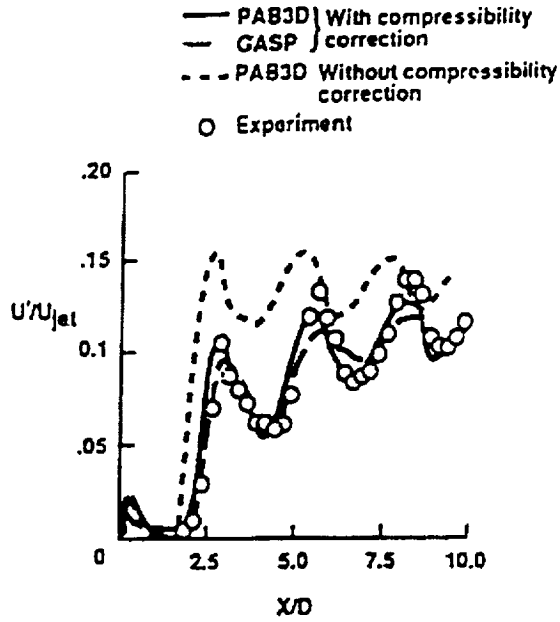

Fig. 16 Lipline turbulence intensity for an underexpanded supersonic jet. -- after Balakrishnan and Abdol-Hamid [57].

Renormalization group (RNG) theory [58] based k-ε model was incorporated into NPARC code by Papp and Ghia [59]. They compared the solutions obtained with the RNG based k-ε model with that of Chien's model [39]. They found that while RNG model produced slightly better results, the Chien's model exhibited numerical stability problems for certain grid resolutions. RNG method appeared to be more robust.

Tubofan engine exhaust nozzle flows [60] and lobed mixer nozzle flows [61] have been successfully calculated with standard k-ε model.

4.3 Algebraic Stress Model (ASM) Prediction

Now with the ability to use axisymmetric turbulence characteristics to compute noise established [9] it is imperative that the Reynolds stress components should be calculated accurately. Algebraic stress model provides that possibility. An example of ASM model prediction of a coaxial jet flow [62] is shown in Fig. 17 and 18. The figures show u' and v' profile variations with axial distance respectively. The ratio of turbulence intensities, $\Delta_u = u_2^2/u_1^2$ and the ratio of transverse to longitudinal length scales can now be calculated accurately for use in the axisymmetric turbulence model for noise calculation [9].

4.4 Reynolds Stress Transport Equations Model Prediction

This model can be used to compute the Reynolds stress components accurately. This model requires modeling of higher order correlations and additional computational efforts to solve the transport equation for each component of the Reynolds stress. For those reasons this model is not as widely used as one would like to be. Figure 19 shows the three components of normal stress profiles in a round jet, computed using the Reynolds stress transport equation model [22].

V. LOCATION OF INLET BOUNDARY AND BOUNDARY CONDITIONS

The inlet boundary condition specification plays a crucial role in turbulence model predictions [63,64]. One can locate the inlet boundary for the jet flow calculations at the jet exit and specify the inlet conditions there, as for example was done by Thies and Tam [51]. Such a choice, avoids the complexities associated with the boundary region such as the near wall modeling and wall limiting behavior of turbulence quantities. However, formodern complex and novel designs such as those with internal mixing device, ejector, etc. the jet exit flow conditions can not easily be generated accurately (or known from measurements). In such complex nozzle flow cases, the nozzle internal flow has to be computed with appropriate near-wall modeling in the nozzle-mixer-elector flow path. Chien's model [39] has been used successfully [6,9] for several jet flow configurations. But, it is essential to incorporate correct wall limiting behavior turbulence quantities by employing a model such as that of Myong and Kasagi [35]. The use algebraic Reynolds stress model (ASM) will provide an accurate description of Reynolds stress components [62].

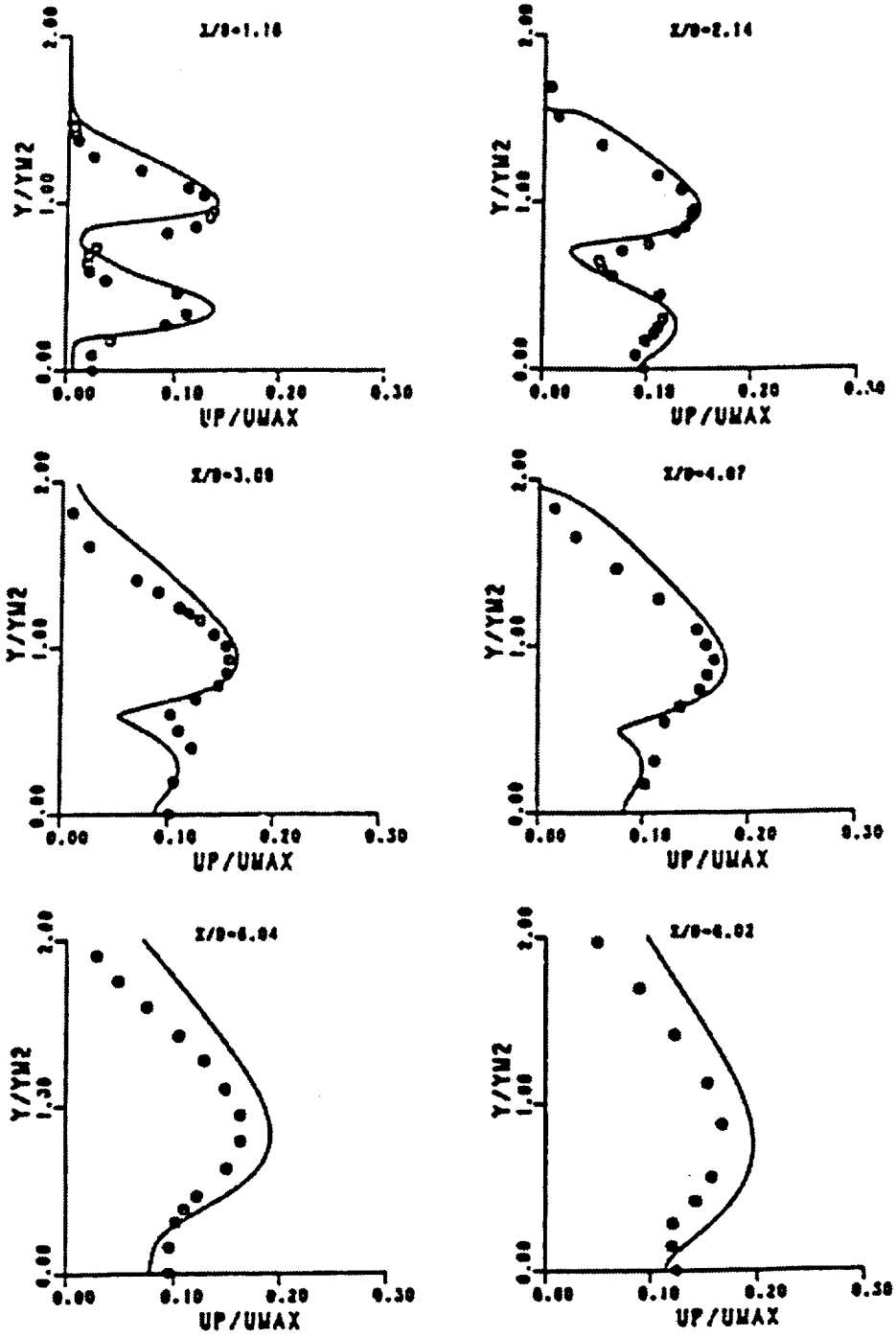

Fig. 17 Predicted and measure profiles of RMS axial velocity, u, for coaxial Jets in ambient air. – after Srinivasan et al [62].

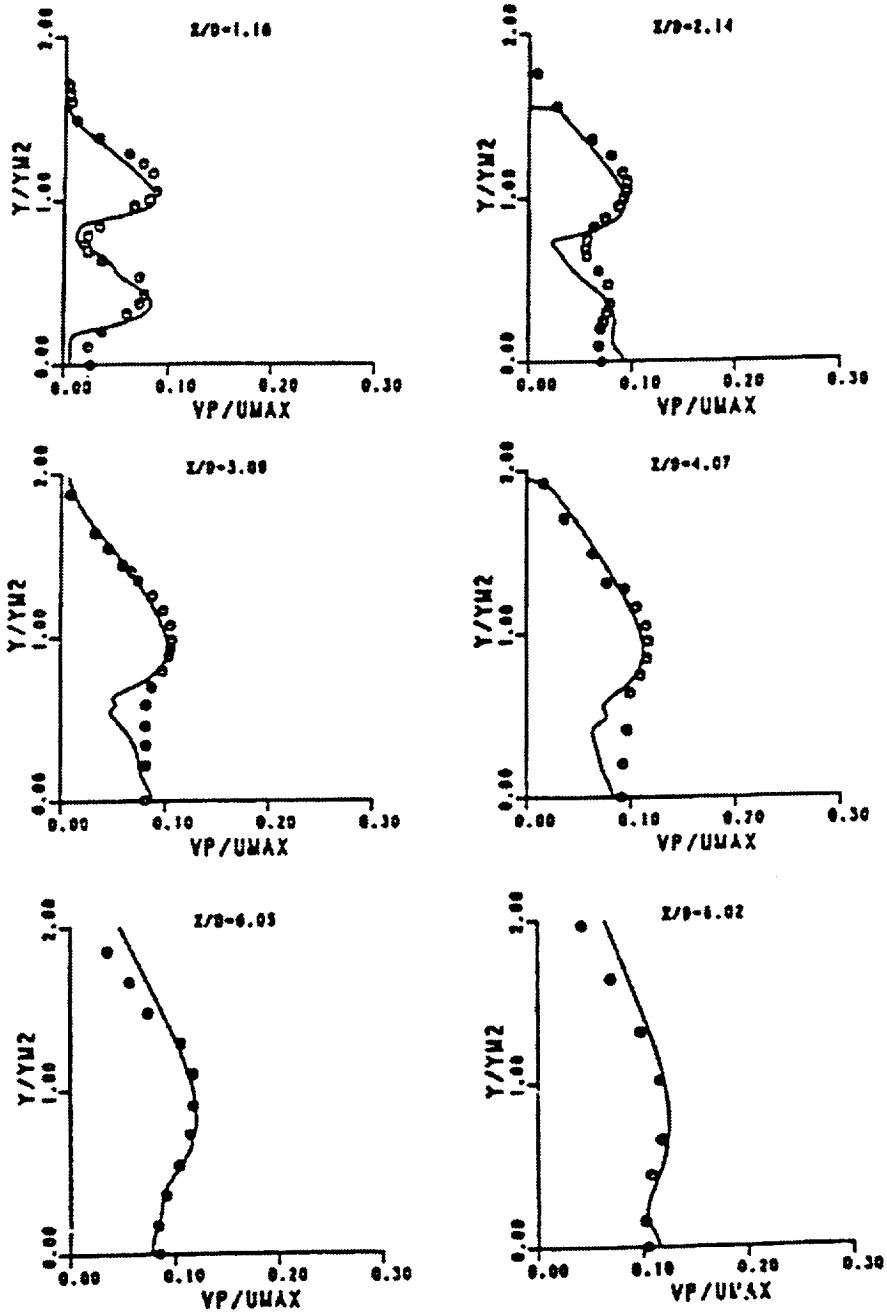

Fig. 18 Predicted and measured profiles of fluctuating radial velocity component, v, in Coaxial jets. – after Srinivasan et al [62].

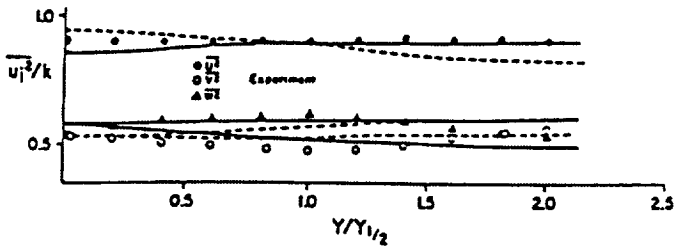

Fig. 19 Normal stress profiles in round jets, — usual thin shear flow form, - - - - including secondary production terms. – after Launder and Morse [22].

VI. NUMERICAL SOLUTION ALGORITHM AND TURBULENCE MODEL

Studies have shown that the same turbulence model incorporated into different codes produce different turbulence characteristics [57,59,65,66]. This may arise due to several factors such as the numerical solution algorithm, grid dependence, turbulence model methodology and implementation, and near-wall model. Flow solvers and turbulence models need careful bench mark testing for jet flow computations so that they can be used with confidence for acoustic assessment of new nozzle designs.

VII. CONCLUDING REMARKS

A brief account of turbulence models that are relevant to provide turbulence characteristics needed for jet mixing noise calculations is presented. Length and time scales should be predicted accurately to estimate the sound pressure levels correctly. The use of compressibility correction due to Sarkar results in correct spreading rates in supersonic jets. For axisymmetric configurations, vortex stretching parameter correction due to Pope provides the correct jet spreading rate. It is recommended that a near-wall model that produces correct wall-limiting behavior of Reynolds stress components be used. Anisotropic turbulence information should be incorporated in the small scale mixing noise calculation to improve the far-filed noise level estimates and spectral distribution.

Jet flow computations that present the components of Reynolds stress are scarce (as indicated by sections 4.3 and 4.4). It is perhaps due to the fact there was no immediate use for them. Moreover models such as algebraic stress models and Reynolds stress transport models were mostly used for complex flows such as non-circular duct flows, curved flows, flows with large separated regions, etc. Recently, it has been shown that a knowledge of the magnitudes of the Reynolds stress components is essential for accurate evaluation of jet noise levels [7,9]. Turbulence models that can provide the distribution of Reynolds stress components must now be considered for jet flow computations. In this regard, algebraic stress models and Reynolds stress transport models are good candidates. Reynolds stress transport models involve substantially more modeling, and

computational effort and time compared to algebraic stress models (section 2.1). Hence, it is recommended that an algebraic Reynolds stress model be implemented in the flow solvers (such as NPARC code) and validated. Anisotropic turbulence characteristics obtained using such a turbulence model would substantially improve the confidence levels in jet mixing noise predictions.

VIII. REFERENCES

1. Lighthill, M.J., "On Sound Generated Aerodynamically. I General Theory," Proceedings of Royal society of London, Vol. A211, 564-587, 1952.

2. Lighthill, M.J., "On Sound Generated Aerodynamically II Turbulence as a source of Sound," Proc. Royal Society of London, A222, 1-32, 1954.

3. Lilley, G.M., "On the Noise from Jets," ARC 20376, 1958.

4. Colonius, T, Lele, S.K., and Moin, P., "Sound Generated in Mixing Layer," J. Fluid Mechanics, Vol. 330, 375-409, 1997.

5. Hinze, J.O., Turbulence, EcGraw-Hill, New York, 1975.

6. Khavaran, A, Krejsa, E.A., and Kim, C.M., "Computation of Supersonic Jet Mixing Noise for Axisymmetric Convergent-Divergent Nozzle," Journal of Aircraft, Vol. 31, 603-609, 1994.

7. Bailly, C., Becharo, W., Lafon, P., and Candel, S., "Jet Noise Predictions using a k-ε Turbulence Model," AIAA Paper 93-4412, 1993.

8. Bailly, C., Lafon, P., and Candel, S., "Computation of Noise Generation and Propagation for Free and Confined Turbulent Flows," AIAA Paper 96-1732, 1996.

9. Khavaran, A., and Krejsa, E.A., On the role of anisotropy in Turbulent Mixing Noise," AIAA Paper 98-2289, 1998.

10. Launder, B.E., and Spalding, D.B., "Turbulence Models and their Applications to the Prediction of Internal Flows," Heat and Fluid Flow, vol. 2, 43-54, 1972.

11. Reynolds, W.C., "Computation of Turbulent Flows," Ann. Rev. Fluid Mech., Vol. 8, 183-208, 1976.

12. Lumley, J.L, "Turbulence Modeling" Adv. Appl. Mech, Vol. 18, 123-176, 1978.

13. Rodi, W., "Examples of Turbulence Models for Incompressible Flows," AIAA J., Vol. 20, 872-879, 1982.

14. Laksminarayana, B., "Turbulence Modeling for Complex Flows," AIAA Paper 85-1652, 1985.

15. Nallasamy, M., " A Critical Evaluation of Various Turbulence Models as Applied to Internal Fluid Flows," NASA-TP -2474, 1985.

16. Hanjalic, K., "Practical Prediction by Single Point Closure Methods - Twenty Years of Experience," In: Near-Wall Turbulence, pp. 762-781. Hemisphere Publishing Corp. New York 1990.

17. Speziale, C.G., "Analytical Methods for the Development of Reynolds Stress Closures in Turbulence," Ann. Rev. Fluid Mechanics, Vol. 23, 107-157, 1991.

18. Wilcox, D.C., "Turbulence Modeling for CFD," 2nd Ed., DCW Industries, 1998.

19. "Industry-Wide Workshop on Computational Turbulence Modeling,", NASA Conference Publication 10165, 1994.

20. Barber, T.J., et al., "High-Speed Civil Transport (HSCT) Nozzle CFD Enhancement Team (NCET) Final Report," 1996.

21. Launder, B.E., Reece, G.J., and Rodi, W., "Progress in the Development of Reynolds Stress Closure," J. Fluid. Mech., Vol. 68, 537-566, 1975.

22. Launder, B.E., and Morse, A., "Numerical Prediction of Axisymmetric Free Shear Flows with a Reynolds Stress Closure," Turbulent Shear Flows, Vol.1, 279-294, 1980.

23. Daly, B.J. and Harlow, F.H., "Transport Equations of Turbulence," Phys. Fluids, Vol. 13, 2634-2641, 1970.

24. Rodi, W., " A New Algebraic Relation for Calculating the Reynolds Stresses," ZAMM Vol. 56, T219-T221, 1976.

25. Launder, B.E., and Spalding, D.B., Mathematical Models of Turbulence, Academic Press, London, 1972.

26. Launder, D.B, and Spalding, D.B., "The Numerical Computation of Turbulent Flows," Comput. Meth. Appl. Mech. Engng., Vol. 3, 269-289, 1974.

27. Hanjalic, K., and Launder, B.E., " A Reynolds Stress Model of Turbulence and its Application to Thin Shear Flows," J. Fluid. Mech., Vol. 52, 609-638, 1972.

28. Pope, S.B., "An Explanation of the Turbulent Round Jet/Plane Jet Anomally," AIAA Journal, Vol. 16, 279-281, 1978.

29. Papamoschou, D., and Roshko, A., "The Compressible Shear Layer: An Experimental Study," J. Fluid Mech., Vol. 197, 453-477, 1988.

30. Sarkar, S., Erlebacher, G, Hussaini, M.Y., and Kreiss, H.O., "The Analysis and Modeling of Dilatational Terms in Compressible Turbulence," NASA-CR-181959, 1989.

31. Sarkar, S., and Lakshmanan, B., "Application of a Reynolds Stress Turbulence Model to the Compressible Shear Layer," AIAA Journal, Vol. 29, 743-749, 1996.

32. Sarkar, S., "The Pressure-Dilatation Correlation in Compressible Flows," Phys. Fluids A. Vol. 4, 2674-2682, 1992.

33. Nisizima, S., and Yoshizawa, A., "Turbulent Channel and Cavity Flows Using anisotropic k-ε Model, AIAA J., Vol 25, 414-420, 1987.

34. Speziale, C.G., "On nonlinear k-l and k-ε Models of Turbulence," J. Fluid Mech. Vol 178, 459-475, 1987.

35. Myong, M.K., and Kasagi, N., "Toward an anisotropic k-ε Turbulence Model Taking into Account the Wall Limiting Behavior of Turbulence," In: proc. 3rd International Symposium on Computational Fluid Dynamics, Nagoya, Japan, 269-274, 1989.

36. Jones, W.P., and Launder, B.E., "The Prediction of Laminarization with Two Equation Model of Turbulence," Int. J. Heat Mass Transfer, Vol. 15, 301-314, 1972.

37. Patel, V.C., Rodi, W., and Scheurer, G., "Turbulence Models for Near Wall and Low Reynolds Number Flows: A Review," AIAA J., Vol. 23, 1308-1319, 1985.

38. Launder, B.E., and Sharma, B.I., "Application of the Energy Dissipation Model of Turbulence to the calculation of flow near a Spinning Disk," Lett. Heat Mass Transfer Vol. 1, 131-138, 1976.

39. Chien, K.Y., "Prediction of Channel and Boundary Layer Flows with a Low Reynolds number Turbulence Model," AIAA J., Vol. 20, 33-38, 1982.

40. Hanjalic, K., Launder, B.E., and Schistel, R., "Multiple-time-scale concepts in Turbulent Transport Modeling," Proc. Turbulent Shear Flows, Vol. 2, 10.31-10.36, 1979.

41. Kim, S,W., and Chen, C.P., "A Multiple Scale Turbulence Model Based on Variable Partitioning of Kinetic Energy Spectrum," NASA-CR-179222, 1987.

42. Chen, C.P., "A non-isotropic Multiple Scale Turbulence Model," NASA-CR-184217, 1990.

43. Duncan, B.S., Liou, W.W., and Shih, T.H., "A Multiple-Scale Turbulence Model for Incompressible Flow," NASA TM-106113, 1993.

44. Ko, S.H., and Rhode, D.L., "Derivation and Testing of a New Multi-Scale k-ε Turbulence Model," AIAA Paper 90-0243, 1990.

45. Reichardt, H., "On a New Theory of Free Turbulence," Royal aeronautical Society J., 167-176, 1943.

46. Berman, C.H., "direct Computation of Turbulence Noise," Final Report, Aerochem TP-475, 1988.

47. Cooper, G.K., and Sirbaugh, J.R., "PARC Code: Theory and Usage," Arnold Engineering Development Center, AEDC-TR-89-15, 1989.

48. Ribner, H.S., "Quadrupole Correction Governing the Pattern of Jet Noise," J. Fluid Mech., Vol. 38, 1-24, 1969.

49. Goldstein, M.E., and Rosenbaum, B., "Effect of Anistropic Turbulence on Aerodynamic Noise," J. Acoustical Soc. of America, Vol. 54, 630-645, 1973.

50. Ffowcs-Williams, J.E., and MaidaniK, G, "The Mach Wave Field Radiated by Supersonic Turbulent Shear Flows," J. Flid Mech., Vol. 21, 641-657, 1965.

51. Thies, A.T., and Tam, K.W., "Computation of Turbulent Axisymmetric and Non-axisymmetric Jet Flows Using the k-ε Model," AIAA J., Vol. 34, 309-316, 1996.

52. Dash, S.M., Sinha, N, and Kenzakowski, d.C., "The Critical Role of Turbulence Modeling in the Prediction of Supersonic Jet Structure for Acoustic Applications," DGLR/AIAA Paper 92-02-106, 1992.

53. Dash, S.M., Kenzakowski, D.C., Seiner, J.M., and Bhat, T.R.S., "Recent Advances in Jet Flow Field Simulation Part I - Steady Flow," AIAA Paper 93-4390, 1993.

54. Dash, S.M., and Kenzakowski, D.C., "Future Directions in Turbulence Modeling for Jet Flow Field Simulation," AIAA Paper 96-1775.

55. Zeman, O., "Dilatational Dissipation: the Concept and Application in Modeling Compressible Mixing Layers," Physics Fluids A, Vol. 2, 178-188, 1990.

56. Seiner, J.M., Penton, M.K., Jansen, B.J, and Lagen, N.T., "The Effects of Temperature on Supersonic Jet Noise Emission," DGLR/AIAA Paper 92-02-046, 1992.

57. Balakrisnan, L., and Abdol-Hamid, K.S., "A Comparative Study of Two Codes with an Improved Two-Equation Turbulence Model for Predicting Jet Plumes," AIAA Paper 92-2604, 1992.

58. Yahkot, V., Orszag. S, Thangam, S., Galski, T.B., and Speziale, C.G., "Development of Turbulence Models for Shear Flows by a Double Expansion Technique," Phys. Fluids A, Vol.4, 1510-1520, 1992.

59. Papp, J.L., and Ghia, K.N., "Study of Turbulent Compressible Mixing Layers Using Two-Equation Turbulence Models Including a RNG k-ε Model," AIAA Paper 98-0320.

60. Birch, S.F., Paynter, G.C., Spalding, D.B., and Tatchell, D.G., "Numerical Modeling of Three Dimensional Flows in Turbofan Engine Exhaust Nozzles," J. Aircraft, Vol, 15, 489-496, 1978.

61. Koutmos, p., and McGuirk, J.J., "Velocity and Turbulence Characteristics of Isothermal Lobed Mixer Flows," In; Proc. Seventh Symposium on Turbulent Shear Flows, 13-5.1 - 13-5.6, 1989.

62. Srinivasan, R., Reynolds, R., Bell, I., Berry, R., Johnson, K., and Mongia,H., "Aerothermal Modeling Program, Phase I Final Report," NASA-CR-168243.

63. Nallasamy, M., and Chen, C.P., "Studies on Effects of boundary conditions in Confined Turbulent Flow Predictions," NASA CR-3929, 1985.

64. Nallasamy, M., "Computation of Confined Turbulent Coaxial Jet Flows," J. Propulsion and Power, Vol. 3, 263-268, 1987.

65. Woodruf, S.L., Seiner, J.M., Hussaini, M.Y., and Erlbacher, G., "Evaluation of Turbulence –Model Performance as Applied to Jet Noise Prediction," AIAA Paper 98-0083.

66. Papp, J.L., and Ghia, K.N., "Implementation of an RNG k-ε Model into Version 3.0 of the NPARC 2-D Navier-Stokes Flow Solver," AIAA Paper 98-0956, 1998.

REPORT DOCUMENTATION PAGE

Form Approved
OMB No. 0704-0188

1. AGENCY USE ONLY (*Leave blank*)	2. REPORT DATE	3. REPORT TYPE AND DATES COVERED
	March 1999	Final Contractor Report

4. TITLE AND SUBTITLE

Survey of Turbulence Models for the Computation of Turbulent Jet Flow and Noise

5. FUNDING NUMBERS

WU-538-03-11-00
NAS3-98008

6. AUTHOR(S)

M. Nallasamy

7. PERFORMING ORGANIZATION NAME(S) AND ADDRESS(ES)

Dynacs Engineering Co.
2001 Aerospace Parkway
Brook Park, Ohio 44142

8. PERFORMING ORGANIZATION REPORT NUMBER

E-11568

9. SPONSORING/MONITORING AGENCY NAME(S) AND ADDRESS(ES)

National Aeronautics and Space Administration
John H. Glenn Research Center at Lewis Field
Cleveland, Ohio 44135-3191

10. SPONSORING/MONITORING AGENCY REPORT NUMBER

NASA CR—1999-206592

11. SUPPLEMENTARY NOTES

Project Manager, Dennis Huff, Glenn Lewis Research Center, organization code 5940, (216) 433-3913.

12a. DISTRIBUTION/AVAILABILITY STATEMENT

Unclassified - Unlimited
Subject Categories: 02 and 71 Distribution: Nonstandard

This publication is available from the NASA Center for AeroSpace Information, (301) 621-0390.

12b. DISTRIBUTION CODE

13. ABSTRACT ***(Maximum 200 words)***

The report presents an overview of jet noise computation utilizing the computational fluid dynamic solution of the turbulent jet flow field. The jet flow solution obtained with an appropriate turbulence model provides the turbulence characteristics needed for the computation of jet mixing noise. A brief account of turbulence models that are relevant for the jet noise computation is presented. The jet flow solutions that have been directly used to calculate jet noise are first reviewed. Then, the turbulent jet flow studies that compute the turbulence characteristics that may be used for noise calculations are summarized. In particular, flow solutions obtained with the k-e model, algebraic Reynolds stress model, and Reynolds stress transport equation model are reviewed. Since, the small scale jet mixing noise predictions can be improved by utilizing anisotropic turbulence characteristics, turbulence models that can provide the Reynolds stress components must now be considered for jet flow computations. In this regard, algebraic stress models and Reynolds stress transport models are good candidates. Reynolds stress transport models involve more modeling and computational effort and time compared to algebraic stress models. Hence, it is recommended that an algebraic Reynolds stress model (ASM) be implemented in flow solvers to compute the Reynolds stress components.

14. SUBJECT TERMS	15. NUMBER OF PAGES
Turbulence models; Jet flow; Jet noise	39
	16. PRICE CODE A03

17. SECURITY CLASSIFICATION OF REPORT	18. SECURITY CLASSIFICATION OF THIS PAGE	19. SECURITY CLASSIFICATION OF ABSTRACT	20. LIMITATION OF ABSTRACT
Unclassified	Unclassified	Unclassified	